

Investigation of electrical and structural properties of Ag/TiO₂/n-InP/Au Schottky diodes with different thickness TiO₂ interface

Ahmet Kürşat Bilgili (✉ ahmet.kursat.bilgili@gazi.edu.tr)

Gazi Üniversitesi

Rabia Çağatay

Gazi Üniversitesi

Mustafa Kemal Öztürk

Gazi Üniversitesi: Gazi Üniversitesi

Metin Özer

Gazi Üniversitesi: Gazi Üniversitesi

Research Article

Keywords: Schottky, structural, electrical, n-InP, TiO₂

Posted Date: February 24th, 2021

DOI: <https://doi.org/10.21203/rs.3.rs-233916/v1>

License:  This work is licensed under a Creative Commons Attribution 4.0 International License.

[Read Full License](#)

Version of Record: A version of this preprint was published at Silicon on April 3rd, 2021. See the published version at <https://doi.org/10.1007/s12633-021-01093-5>.

Investigation of electrical and structural properties of Ag/TiO₂/n-InP/Au Schottky diodes with different thickness TiO₂ interface

Ahmet Kürşat Bilgili¹, Rabia Çağatay¹, Mustafa Kemal Öztürk², Metin Özer¹

¹Gazi University, Physics Department, 06550, Teknikokullar, Ankara, Turkey

²Gazi University, Photonics Research and Application Center, 06550, Teknikokullar, Ankara, Turkey

Abstract

In this study, structural and electrical properties of Ag/TiO₂/n-InP/Au Schottky barrier diodes are investigated. Particle size, d- spacing, micro-strain, ideality factor and barrier heights of two samples are determined for two different interfacial TiO₂ layer thickness. X-ray diffraction (XRD) and current-voltage (I-V) measurements are employed for mentioned parameters. It is seen that sample with 60 Å TiO₂ interfacial layer is a more ideal diode. The reason for this is argued in main text and conclusion section.

Key words: Schottky, structural, electrical, n-InP, TiO₂

Corresponding author e-mail address: ahmet.kursat.bilgili@gazi.edu.tr

1. Introduction

Investigation of electric and structural properties of solid-state materials started in the beginning of 1800s. As a result of these investigations and experiments these materials are classified according to their electric conductivity. This classification is made in terms of carrier densities (holes and electrons) in valance and conduction bands of solid-state materials. Band gaps, regions without electrons, maintains data on type of material and helps to classify them as conductor, semiconductor or insulator. Band structure of a material gives light to its electric, magnetic and optic properties.

In semiconductors, forbidden region between valance and conduction bands is very narrow and current can be created with a small external energy. Conductivity of semiconductor material is dependent on electric field, impurity, temperature, magnetic field and intensity of luminance.

Because electric properties of semiconductors can be modified by doping impurities to crystal structure or applying external light and electric field, devices made up of semiconductors can be used for amplification, trigger circuits or energy conversion. By adding different type of materials and combining doped semiconductors with different properties, diodes and transistors are constructed. These devices are fundamentals of modern electronics.

Electronic technology today includes use of semiconductor materials. For instance, in laptops, scanners, cell phones etc. mass production of semiconductor integrated circuits is obliged. By high technology, in electronics industry semiconductors are investigated after combining with metals. Combination of semiconductor and metal is called as Schottky diode. Schottky diode is an electronic combination also known as barrier diode. It is used commonly as a rectifier in radio frequency and power applications. Schottky diode is a semiconductor diode which has a small voltage drop in forward bias. This small voltage drop gives opportunity to faster triggering and better system efficiency.

Also, Schottky barrier diodes form base of photodetectors, solar cells and metal-semiconductor transistors[1, 2]. Two of the fundamental properties of Schottky barrier diodes are barrier height (Φ_B) and ideality factor (n). Value of Φ_B is dependent on combination of metal and semiconductor[3].

Metal-semiconductor contacts formed by using InP semiconductor have less stability level according to other contacts formed with different semiconductors because of low barrier height and large reverse bias leak current[4]. In order to overcome this instability problem surface passivations are made with different solutions. As a result of these passivations more optimised surfaces are gained[5]. After these experiments contact studies with InP semiconductors are made by forming an interface layer between metal and semiconductor layers[6]. Korucu et al. noticed that in Au/n-InP Schottky barrier diodes ideality factor decrease and barrier height increase with increasing temperature. They attributed this result to inhomogenities in barrier height, interface states and effect of series resistance.

There are a few studies for both electrical and structural properties of Schottky structures. For example Reddy et al. investigated No/n-GaN Schottky diodes and found that interface could be the reason for degradation of Schottky diode[7]

TiO₂ (Titanium di oxide) is a metal oxide formed by combination of Ti(Titanium) and oxygen. It is used in optic applications with its wide band gap (3 eV) and high refractive index ($n=2.3$).It is frequently used in solar panels, self-cleaning surfaces, treatment of cancer, photovoltaic devices. One more advantage of TiO₂ is low cost and easy production.

In this study TiO₂ is used as interface layer. Both structural and electric properties of *Ag/TiO₂/n-InP/Au* Schottky barrier diode are investigated.

2. Experimental

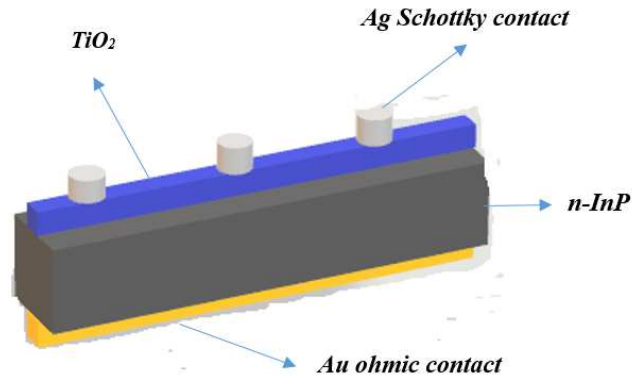


Figure 1. Schematic diagram of Ag/TiO₂/n-InP/Au Schottky barrier diode

In this study Ag/TiO₂/n-InP/Au Schottky structure is constructed by using sputtering method on chemically cleaned n-InP semiconductor. n type InP semiconductor crystal is used with (100) orientation, 500 μm thickness and $3.13 \times 10^{18} \text{ cm}^{-3}$ carrier density as a wafer. At first step n-InP crystal is cut with a diamond cutter and two wafers are formed. Ohmic contact is formed on rough side of the samples. TiO₂ thin film is grown on polished side of the wafers with 60 Å and 120 Å thicknesses and two different samples are gained. In the following sections of this study, samples with 60 Å and 120 Å thicknesses will be mentioned as sample A (S.A) and sample B (S.B), respectively.

Cleaning procedure:

In order to construct a well optimised MS diode qualified and chemically well cleaned crystals should be used. Wafers are cleaned chemically in ultrasonic bath to remove organic and heavy metal impurities on their surfaces by following different steps. During cleaning of wafers deionised water (18.3 MΩ) (DIW) is used. Because cleaning of wafers and other experimental tools is very important to form a good performance Schottky diode all chemical operations are made very sensitively. In cleaning procedure ordered steps are followed:

- 1- All glass beakers and tweezers are cleaned with DIW and dried in high temperature oven.
- 2- Steps during cleaning of iron mask, tweezers and wafers (n-InP) are given below:
 - a- Washing in ultrasonic bath with trichloroethylene for 5 minutes.
 - b- Rinsing with DIW
 - c- Washing in ultrasonic bath with acetone for 5 minutes.
 - d- Rinsing with DIW.

- e- Washing in ultrasonic bath with methanole for 5 minutes.
- f- Rinsing with DIW.
- g- At the end of rinsing, in order to remove natural oxide layer on the surface wafers are waited in (1:10) HF+H₂O solution for 30 seconds.
- h- Rinsed with DIW.
- i- Tweezers, masks and wafers are dried in high purity N₂ atmosphere.

Formation of ohmic contact:

After chemical cleaning and drying operations, in order to form Au ohmic contact on the rough side of wafers, samples are attached to sputtering system. System is vacumed to (2×10^{-6} Torr). Pure Au (%99.995) is sputtered on rough side of wafers with a thickness of 150 nm. During this sputtering operation temperature is kept constant at 80 °C. To form ohmic contact samples are annealed at 325 °C for 4 minutes.

Sputtering system operates as follows: wafers are put in sputtering system. Air in sputtering system is vacumed until desired pressure. Target metal is charged negatively. An electric field occurs with this negative charging resulting with a plasm medium. Positively charged gas ions comes out in this plasm medium and they hit the target metal with a big momentum. Atomic particles of target metal leaves it as a result of momentum transfer. These atomic particles pass through vacuum region and they stick on wafer surface.

Formation of Schottky contact:

In O₂ atmosphere Ti is sputtered on polished side of samples. 60 Å and 120 Å thick TiO₂ thin films are formed on polished sides of samples. Ag is coated on this interface with sputtering method with a thickness of 1500 Å to form Schottky contacts. During coating procedure an iron mask is used to gain 1mm radius diodes.

3. Results and Discussion

X-ray analysis of both samples are made with Bruker D8-Discover HRXRD device that contains Ge(220) oriented four crystal monocromator and X-ray source tube that produce 1.540 Å CuK_{α1} wavelength X-rays. w- 2θ scanning of both samples are made for (002) plane. In Figure 2 X-ray diffraction patterns for S.A and S.B can be seen.

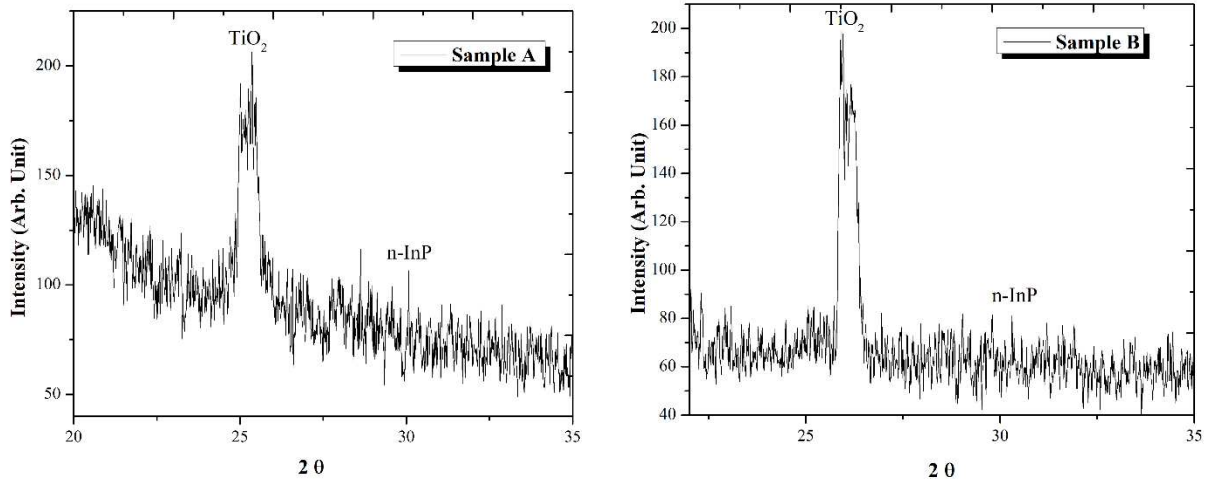


Figure 2. XRD patterns for S.A and S.B

In literature in classical calculations, 2θ angle is kept constant and rocking curve results are used by detecting θ angle[8, 9, 10]. But many factors are effective in optimising rocking curves. Surface bending, adjusting sample height, azimuthal modifications are some of the modifications needed to be optimised. Making device adjustments crystallographically well, optimisation based errors can be reduced and parameters of samples can be gained accurately[11].

As can be seen in Figure 2 for S.A peak positions of n-InP and TiO_2 are determined as 30.068 and 25.368 respectively. Full width at half maximum (FWHM) values are found as 0.02 for both layers in S.A. The same parameters for S.B are determined as 30.308 and 25.898. FWHM values for S.B are 0.04 and 0.089 for n-InP and TiO_2 layers respectively. FWHM values and peak positions are determined with peak analysis method by using a convenient software. As can be noticed if thickness of interface increase there is a positive shift in peak positions. So thickness of interface effects Bragg reflections. This situation may stem from lattice condensation with increasing thickness.

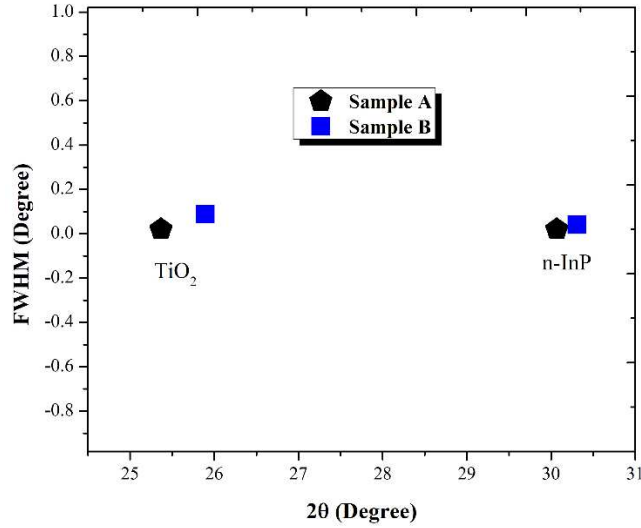


Figure 3. Variation of FWHM with 2-theta for S.A and S.B

In Figure 3 variation of FWHM versus 2-theta plot can be seen. As can be seen in Figure 3 there is a shift in FWHM values dependent on 2-theta with increasing interface thickness. Shift in TiO₂ layers is larger than n-InP layers. This may be because n-InP wafer is a template.

Crystallite size and d-spacing of n-InP and TiO₂ layers are determined by using Bragg formula and Scherrer method. In order to apply Scherrer method safely, FWHM value should be determined accurately[12].

Crystallite size normal to reflective planes D can be gained by using equation (1)

$$D = \frac{k\lambda}{\beta_{hkl} \cos \theta} \rightarrow \cos \theta = \frac{k\lambda}{D} \left(\frac{1}{\beta_{hkl}} \right) \quad (1)$$

Here k is a coefficient, λ is wavelength of X-ray and θ is Bragg angle. d- spacing can be determined by using classic Bragg formula given in equation (2).

$$2d \sin \theta = n\lambda \quad (2)$$

If we insert 1 in n we found d-spacing of atoms in lattice in other words we determine first degree reflection result. Results gained from these two equations are given in Table 1 for n-InP and TiO₂ layers.

Table 1. Particle size and d-spacings of n-InP and TiO₂ layers in S.A and S.B

	S.A		S.B	
(nm)	Particle size	d-spacing	Particle size	d-spacing
n-InP	80.063	1.537	80.258	1.526
TiO₂	76.687	1.798	77.027	1.763

All values gained for these two samples are in good accordance with previous works done by different researchers in literature. Also micro-strain values for both n-InP and TiO₂ layers are calculated for S.A and S.B by using equation (3). [12]

$$\varepsilon = \frac{\beta_{hkl}}{4 \tan \theta} \quad (3)$$

Strain is a result of imperfect crystal structure. In equation (3) ε is root mean square (RMS) value of micro strain. Micro strain values are determined as 0.0086 and 0.0105 for n-InP and TiO₂ layers in S.A. For S.B micro strain values are determined as 0.017 and 0.045 for n-InP and TiO₂ layers respectively.

Here strain is assumed as uniform in all crystallographic orientations. It is assumed that crystal is isotropic and all parameters are independent of measured plane.

Dielectric (oxide) layer between metal and semiconductor converts metal-semiconductor (MS) structure to metal-insulator-semiconductor (MIS) structure. As thickness of this interfacial layer increase interface states starts to be in equilibrium with semiconductor. This situation effects structural parameters, interfacial layer, interfacial states and current-voltage (I-V) characteristics. Various current conduction mechanisms such as termionic emission (TE), diffusion, termionic field emission (TFE) may be effective in Schottky structures[13]. For this reason it may be difficult to explain I-V characteristics. I-V plot can be seen in Figure 4.

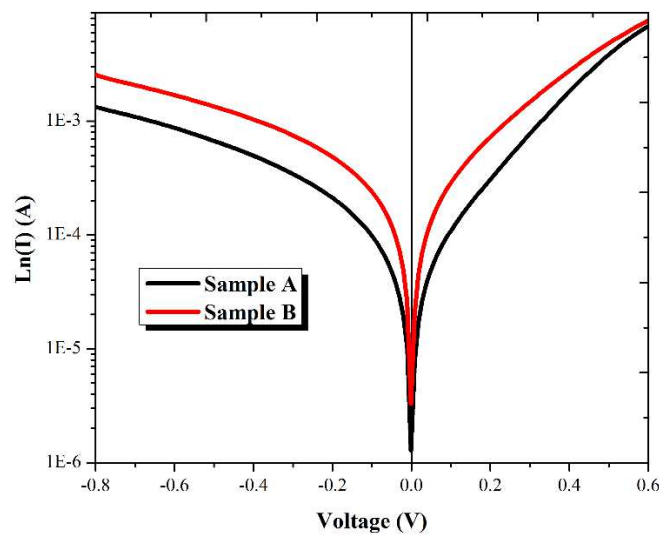


Figure 4. Ln(I) vs Voltage plot for S.A and S.B

In ideal Schottky diodes, current conduction mechanism obeys TE model unless applied voltage is not too high. According to this model current can be defined as in equation (4).

$$I = I_o \left[\exp\left(\frac{qV_D}{kT}\right) - 1 \right] \quad (4)$$

Here V_D is the potential difference on diode, k is Boltzman constant, T is temperature in Kelvin and I_o is saturation current. I_o can be defined as in equation (5).

$$I_o = AA^*T^2 \exp\left[\frac{-q}{kT} \phi_B\right] \quad (5)$$

Here A is diode area, A^* is effective Richardson constant and Φ_B is barrier height[19]. By using equations (4) and (5) $\ln(I) = \ln(I_o) + V_D$ is gained. This is a mathematical definition of a line. Slope of this line gives ideality factor (n). In forward bias region of I-V plot slope of linear part is defined as $\tan\theta = q/nkT$, so ideality factor can be determined with equation (6).

$$n = \frac{q}{kT \tan \theta} \quad (6)$$

Saturation current can be gained from y axis intercept point of semi-logarithmic $\ln(I)$ -V plot. Barrier height Φ_B can be calculated with equation (7)[13].

$$\phi_B = \frac{kT}{q} \ln\left(\frac{AA^*T^2}{I_o}\right) \quad (7)$$

Ideality factors (n) are determined as 1.39 and 1.41 and barrier heights (Φ_B) are determined as 0.52 eV and 0.50 eV for S.A and S.B respectively at room temperature. It is desired that ideality factor is near 1 and barrier height is high for an ideal Schottky diode[10, 25]. So S.A is a more optimised diode. In practice there is no diode with ideality factor equal to 1. Because of oxide layer at interface applied voltage effects barrier height[14,15 ,16, 17]

4. Conclusion

In this study, both structural and electrical properties of Ag/TiO₂/n-InP/Au Schottky barrier diodes are investigated. In structural terms, particle size, d-spacing and microstrain are determined by using data from XRD pattern. Results are given in Table 1 and in main text. In electrical terms from I-V plot ideality factors and barrier heights of samples are determined. It is seen that S.A is a more optimised diode. As thickness of TiO₂ interface decrease diode became more optimised. The reason for this may be series resistance effect that can be seen in

bending of forward bias region in Figure 4. Difference between d-spacings of TiO₂ and n-InP layers for S.A is 0.261 nm and 0.237 nm for S.B. This situation implies that there is larger lattice mismatch between TiO₂ and n-InP layers in S.A. Lattice mismatch may be responsible for decreasing or increasing series resistance along the sample. Vibrating atoms and electron cloud around them may produce extra electric fields on path-way of carriers and gives hand to inhomogeneous barrier height in Schottky structures.

Acknowledgements: This work was supported by Presidency Strategy and Budget Directorate (Grant Number: 2016K121220).

****Funding statement:*** There is no funding source for this resesarch article.

****Conflict of Interest:*** We declare that there is no conflict of interest for this study.

****Author contributions:***Ahmet Kürşat Bilgili(corresponding author), Rabia Çağatay (drawing plots), Mustafa Kemal Öztürk (calculations), Metin Özer (checking and editing).

****Availability of data and material:*** All data used in this research article is available by permission of authors.

****Compliance with ethical standards:*** During formation of this article we obeyed ethical standartars.

****Consent to participate:*** All authors are consent to participate for this study.

****Consent for Publication:*** We declare that we are consent to publish this research article.

References

[1] Ates, A., Saglam, M., Guzeldir, B., Yildirim, M.A. and Astam, A., 2010. The electrical characteristics of cu/cus/p-si/al structure. Journal of Optoelectronics and Advanced Materials, 12(7), 1466-1471.

[2] Aydogan, S., Saglam, M. and Turut, A., 2005. Current-voltage and capacitance-voltage characteristics of polypyrrole/p-inp structure. Vacuum, 77(3), 269-274.

[3] Tung, R.T., 2000. Comment on "numerical study of electrical transport in homogeneous schottky diodes" [j. Appl. Phys. 85, 1935 (1999)]. Journal of Applied Physics, 88(12), 7366-7367.

[4] Cakici, T., Guzeldir, B. and Saglam, M., 2015. Temperature dependent of electrical characteristics of au/n-gaas/in schottky diode with in2s3 interfacial layer obtained by using spray pyrolysis method. Journal of Alloys and Compounds, 646, 954-965.

- [5] Iyer, R. and Lile, D.L., 1991. Role of polysulfides in the passivation of the InP surface. *Applied Physics Letters*, 59(4), 437-439.
- [6] Ayyildiz, E., Cetin, H. and Horvath, Z.J., 2005. Temperature dependent electrical characteristics of Sn/P-Si Schottky diodes. *Applied Surface Science*, 252(4), 1153-1158.
- [7] Reddy, R., Ramesh, K., Choi, C., 2006. Structural and electrical properties of Mo/n-GaN Schottky diodes. *Progress in Materials Science*, Volume 203, Issue 3, Pages 622-627.
- [8] Öztürk, M. K., Yu, H., Sarıkavak, B., Korçak, S., Özçelik, S., Özbay, E. (2010). Structural analysis of an InGaN/GaN based light emitting diode by X-ray diffraction. *Journal of Materials Science: Materials in Electronics*, 21(2), 185-191.
- [9] Öztürk, M. K., Altuntaş, H., Çörekçi, S., Hongbo, Y., Özçelik, S. and Özbay E. (2011). Strain-Stress analysis of AlGaIn/GaN heterostructures with and without an AlN buffer and Interlayer. *Strain*, 47(s2), 19-27.
- [10] Kisielowski, C. (1999). Strain in GaN thin films and heterostructures. *Semiconductors and Semimetals*, 57(GaN II), 275-317.
- [11] Baş, Y. (2015). *In_xGa_{1-x}N (x= 0,075; 0,090; 0,100) Mavi LED'lerin Mikroyapısal Kusurlarının Ters Örgü Uzay Haritası İle İncelenmesi*, Doktora Tezi, Gazi Üniversitesi Fen Bilimleri Enstitüsü, Ankara, 1,2,9,12,14,15,16,24,25,28,34,35,45,46,55.
- [12] G. Singla, K. Singh, O. P. Pandey (2013). Williamson–Hall study on synthesized nanocrystalline tungsten carbide (WC), *Applied Physics A*, 113(1), 237–242.
- [13] Bilgili A. K., Güzel T., Özer M. (2018). Current-voltage characteristics of Ag/TiO₂/n-InP/Au Schottky barrier diodes. *J. Appl. Phys.* 125, 035704 (2019); <https://doi.org/10.1063/1.5064637>
- [14] Sze, S.M., “Physics of Semiconductor Devices 2nd ed.”, *Wiley*, New York, 245 300 (1981)
- [15] Cowley, A.M., Sze, S.M., “Surface State and Barrier Height of Metal ... Semiconductor Systems”, *J. Appl. Phys.*, 36: 3212-3216 (1965).
- [16] Brillson, L.J., “The Surface and Properties of Metal-Semiconductor Interfaces”, *Surf. Sci. Reports.*, 2: 123-326 (1982).
- [17] M. Passlack, N. E. J. Hunt, E. F. Schubert, G. J. Zydzik, M. Hong, J. P.Mannaerts, M. Passlack, R. L. Opila, and R. J. Fischer. ”Dielectric properties of electron-beam deposited Ga₂O₃ films” *Appl. Phys. Lett.*, 64, 20 (1994).

Figures

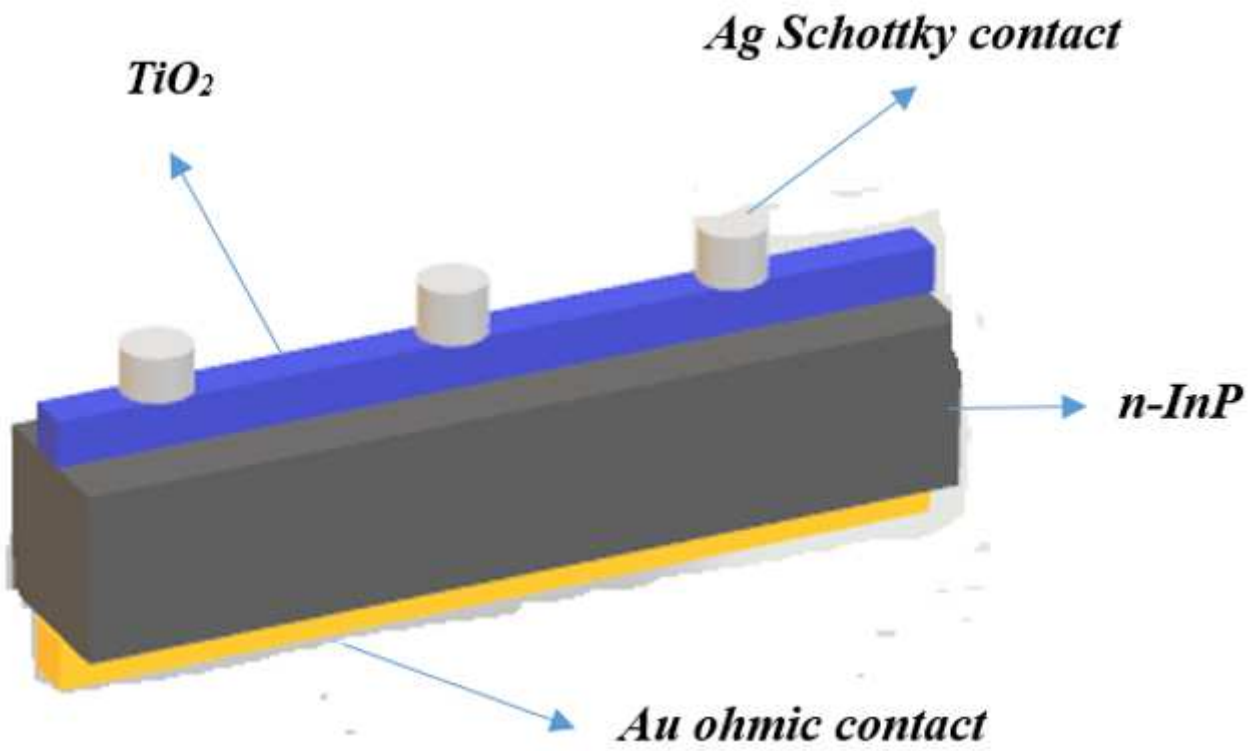


Figure 1

Schematic diagram of Ag/TiO₂/n-InP/Au Schottky barrier diode

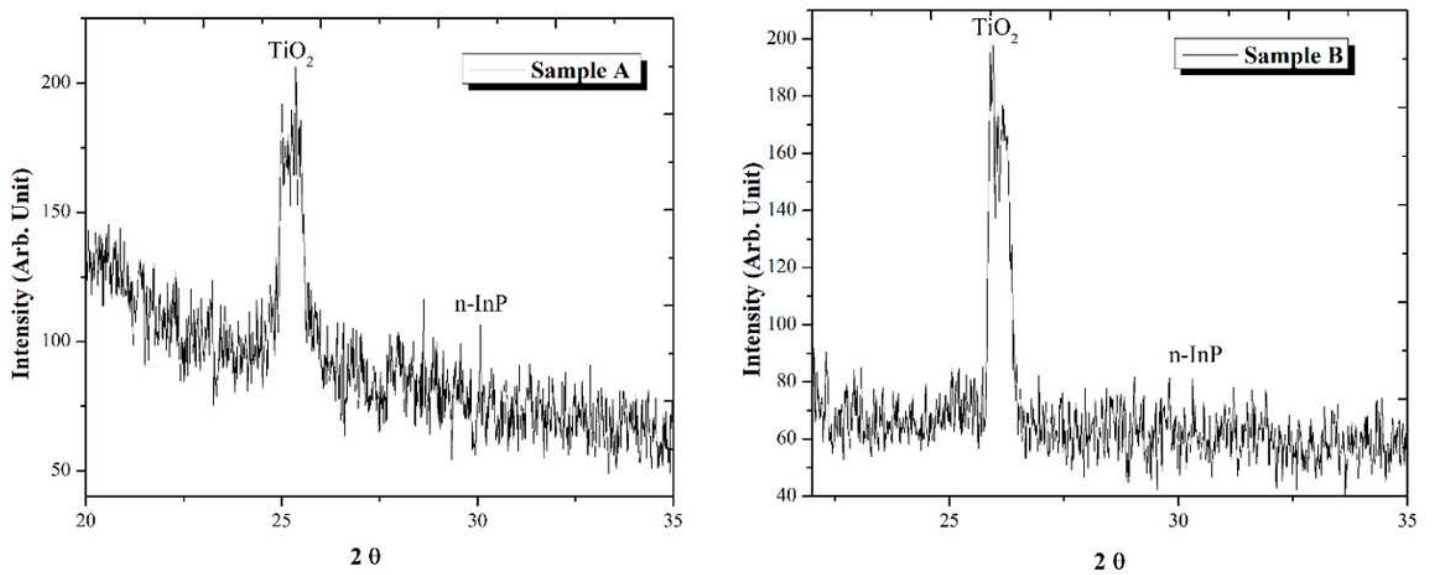


Figure 2

XRD patterns for S.A and S.B

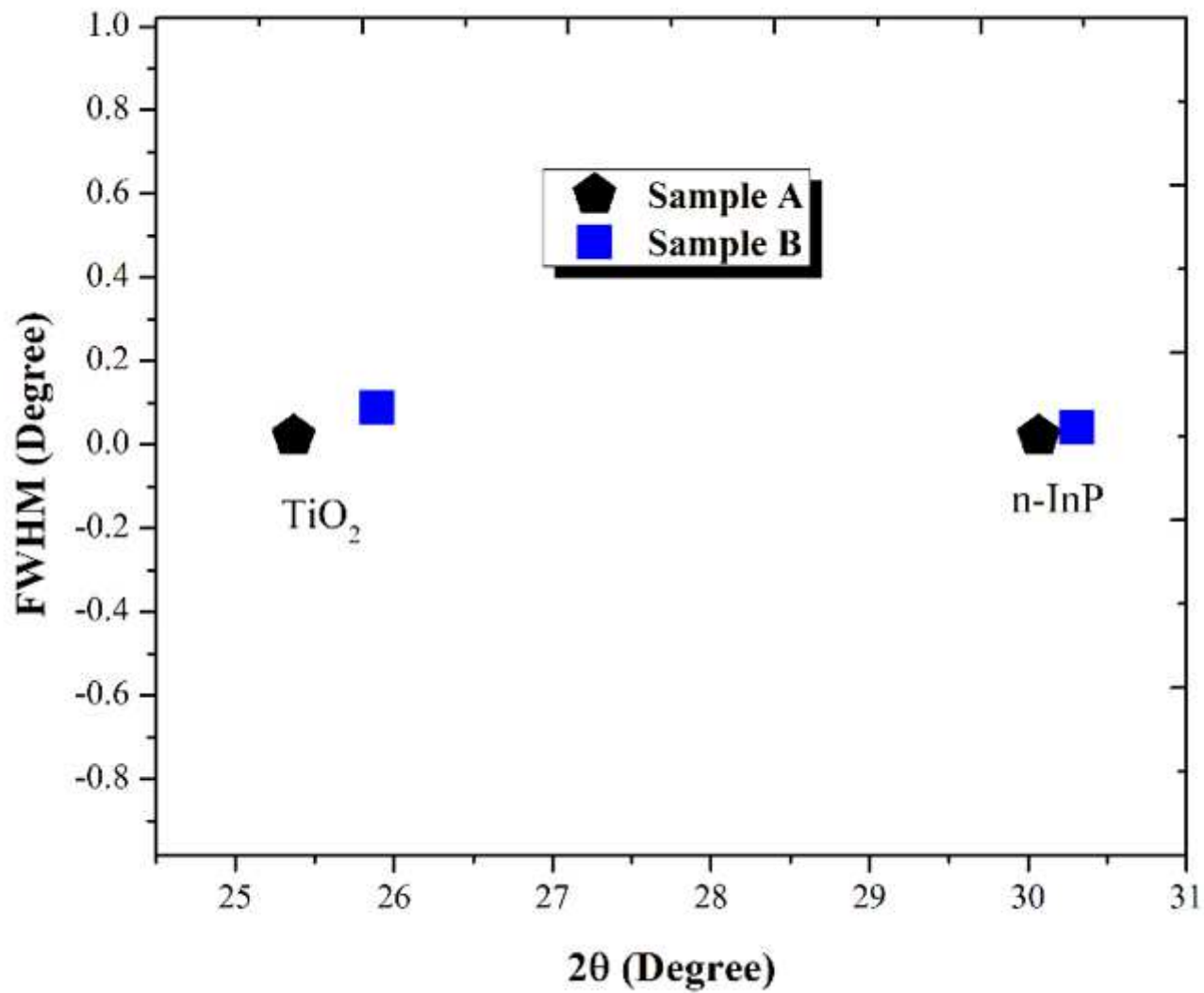


Figure 3

Variation of FWHM with 2-theta for S.A and S.B

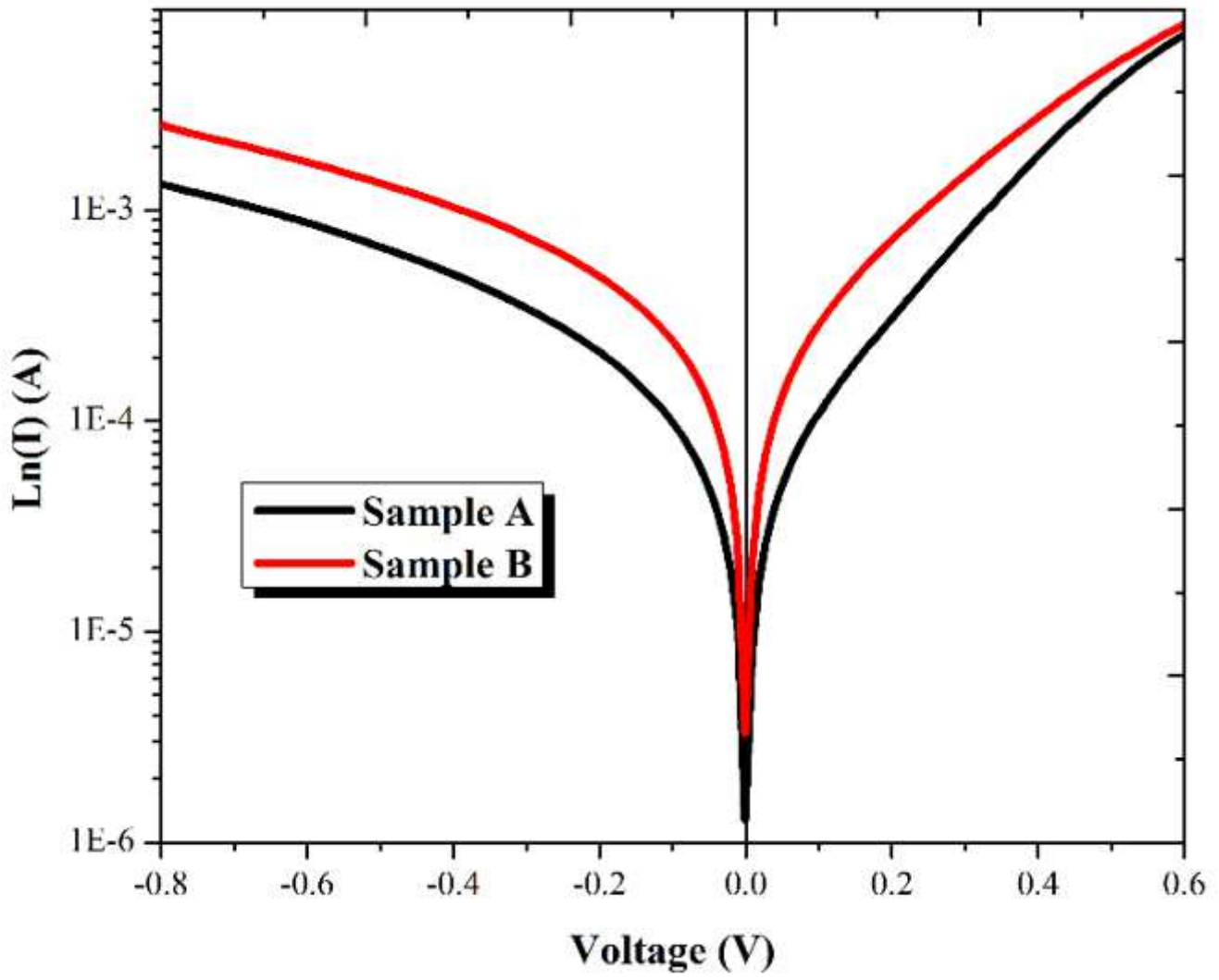


Figure 4

$\text{Ln}(I)$ vs Voltage plot for S.A and S.B